第33卷第1期 红外与毫米波学报 Vol. 33, No. 1
2014年2月 J. Infrared Millim. Waves February, 2014

文章编号：1001－9014(2014)01－0068－04 DOI：10.3724/SP.J.1010.2014.00068

MWIR continuous zoom optical system with magnification of 45

ZHOU Hao[1,2], LIU Ying[1*], SUN Qiang[1], LI Chun[1], ZHANG Xiao-Long[1,2], HUANG Jian-Bo[1]
(1. Changchun Institute of Optics, Fine Mechanics and Physics, Chinese Academy of Sciences, Jilin 130033, China;
2. University of Chinese Academy of Sciences, Beijing 100049, China)

Abstract: The MWIR continuous zoom optical system has many advantages. A method for designing the system with large zoom range was introduced. Then, a system with 8 lenses was designed. The system works in the wavelength range of 3.7～4.8 μm with 10～450 mm continuous zoom, and the MTF value in Nyquist limit (16 lp/mm) is more than 0.3 over the full range. The F/number of the system is 4. It can satisfy 100% cold shield efficiency.

Key words: MWIR; continuous zoom; large zoom range; optical design
PACS: 42.15.Eq

45倍中波红外连续变焦光学系统

周 昊[1,2], 刘 英[1*], 孙 强[1], 李 淳[1], 张晓龙[1,2], 黄剑波[1]
(1. 中国科学院 长春光学精密机械与物理研究所,吉林 长春 130033;
2. 中国科学院大学,北京 100049)

摘要: 红外连续变焦光学系统具有很多优势,介绍了一种可以实现高变焦比的设计方法.据此设计了一个系统,其由八片透镜组成,工作波段为3.7～4.8 μm,可实现10～450 mm连续变焦.系统在全焦距范围内奈奎斯特频率处的MTF值均大于0.3,系统F数为4,且满足冷光阑效率100%的要求.

关 键 词: 中波红外;连续变焦;高变焦比;光学设计
中图分类号: TN216 **文献标识码**: A

Introduction

There are lots of advantages about infrared imaging technology. Infrared optical systems are used in many applications. Continuous zoom optical system has a continuous change in the field of view, searching target in wide field of view while observing target in narrow field of view [1-3]. The demand of infrared continuous zoom optical system increases, especially for those with large zoom range. Large zoom range means that the system has a greater range of search and a higher accuracy of observation, and so there is great significance in design of infrared continuous zoom system with large zoom range. There are two types of zoom systems, optically compensated and mechanically compensated. Almost all infrared zoom systems are mechanically compensated[4]. In a traditional mechanically compensated zoom system, one element move for changes in focal length, while the other one move to eliminate image shift, as shown in Fig. 1. Using traditional mechanically compensated type, MWIR zoom systems can not achieve a large zoom range (such as 45)[1-3, 5-9].

Received date: 2012-12-10, **revised date**: 2013-07-04 **收稿日期**: 2012-12-10, **修回日期**: 2013-07-04
Foudantion item: Supported by the program of academy-locality cooperation of the Chinese Academy of Sciences (2011CJT0004), the Jilin province science and technology development plan item (20090557 and 20125092).
Biography: Zhou Hao (1989-), male, Bozhou Anhui. He is currently pursuing his PhD at the University of Chinese Academy of Sciences. His research interests are infrared optical systems and system evaluation.
* **Corresponding author**: E-mail: ciompzh@hotmail.com.

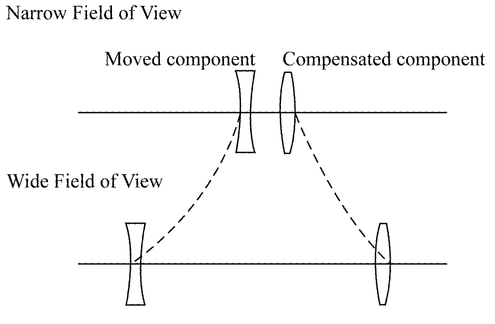

Fig. 1　Traditional mechanically compensated type
图 1　传统机械变焦类型

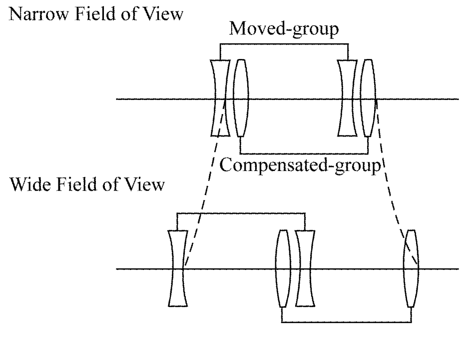

Fig. 2　New mechanically compensated type
图 2　新型机械变焦类型

In this paper, the new mechanically compensated type for continuous zoom system with large zoom range is introduced. In the zoom system, two elements move together for changes in focal length, while two other elements move together to eliminate image shift, as shown in Fig. 2. Especially, the system works with cooled FPA detector. Then a MWIR continuous zoom system was designed. It can realize continuous zoom of 10 ~ 450 mm.

1　Principles

Figure 3 presents schematic of the zoom optical system. In the system, by moving moved components (constituted of M_1 and M_2) and compensated components (constituted of C_1 and C_2), the field of view can be changed continuously. During the process of zooming, elements X_1, X_2 and R are all stable. I_1 is the position of the image focal point of element X_1, I_5 is the position of the image plane of the system.

1.1　Zoom

Figure 4 presents the zoom part of the system composed of thin lenses. H_1 is the position of the primary

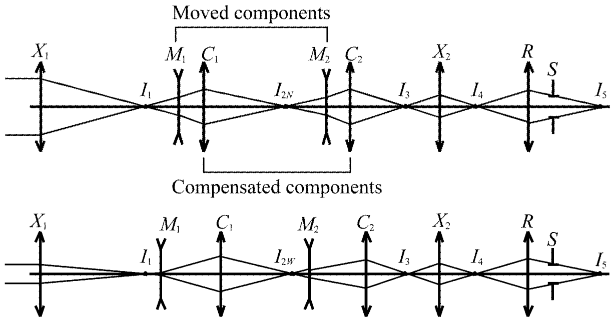

Fig. 3　Schematic of the zoom system
图 3　变焦系统原理图

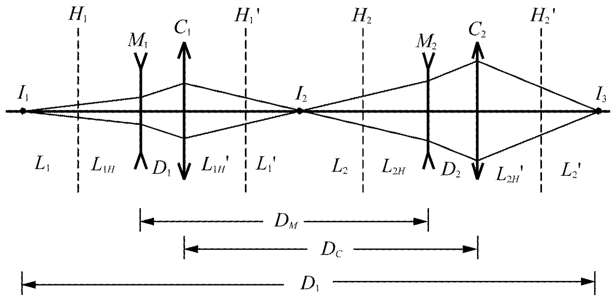

Fig. 4　Scheme of the zoom part
图 4　光学系统变焦部分

principal plane of the two elements M_1 and C_1, H_1' is the position of the secondary principal plane of the two elements M_1 and C_1. H_2 is the position of the primary principal plane of the two elements M_2 and C_2, H_2' is the position of the secondary principal plane of the two elements M_2 and C_2. I_2 is the image of the point I_1, I_3 is the image of the point I_2. D_M is the distance of M_1 from M_2, D_C is the distance of C_1 from C_2, D_I is the distance of I_1 from I_3. The distances are given by relations,

$$D_M = D_1 + L_{1H}' + L_1' - L_2 - L_{2H} \quad , \quad (1)$$

$$D_C = - D_1 + D_M + D_2 \quad , \quad (2)$$

$$D_I = - L_1 - L_{1H} + D_M + D_2 + L_{2H}' + L_2' \quad , \quad (3)$$

where $-L_1$ is the distance of I_1 from H_1, $-L_{1H}$ is the distance of H_1 from M_1, D_1 is the distance of M_1 from C_1, L_{1H}' is the distance of C_1 from H_1', L_1' is the distance of H_1' from I_2, $-L_2$ is the distance of I_2 from H_2, $-L_{2H}$ is the distance of H_2 from M_2, D_2 is the distance of M_2 from C_2, L_{2H}' is the distance of C_2 from H_2', L_2' is the distance of H_2' from I_3. As it is well known [10], the following relations hold for imaging,

$$D_1 = F_{M1} + F_{C1} - \frac{F_{M1} \cdot F_{C1}}{F_1}, L_{1H} = \left(\frac{F_{M1}}{F_{C1}} + 1\right) \cdot$$

$$F_1 - F_{M1}, L_{1H}' = -\left(\frac{F_{C1}}{F_{M1}} + 1\right) \cdot F_1 + F_{C1},$$

$$D_2 = F_{M2} + F_{C2} - \frac{F_{M2} \cdot F_{C2}}{F_2}, L_{2H} = \left(\frac{F_{M2}}{F_{C2}} + 1\right) \cdot$$

$$F_2 - F_{M2}, L_{2H}' = -\left(\frac{F_{C2}}{F_{M2}} + 1\right) \cdot F_2 + F_{C2},$$

$$L_1 = \left(\frac{1}{\beta_1} - 1\right) \cdot F_1, L_1' = (1 - \beta_1) \cdot F_1,$$

$$L_2 = \left(\frac{1}{\beta_2} - 1\right) \cdot F_2, L_2' = (1 - \beta_2) \cdot F_2, \quad (4)$$

where F_{M1} is the focal length of M_1, F_{C1} is the focal length of C_1, F_1 is the focal length of the two elements M_1 and C_1, β_1 is the magnification of the two elements M_1 and C_1, F_{M2} is the focal length of M_2, F_{C2} is the focal length of C_2, F_2 is the focal length of the two elements M_2 and C_2, β_2 is the magnification of the two elements M_2 and C_2. T is the magnification of the zoom part (elements M_1, C_1, M_2 and C_2). From equations (1) ~ (4), we obtain:

$$\frac{F_{C1}}{F_{M1}} \cdot F_1 + \frac{F_{M2}}{F_{C2}} \cdot F_2 + \beta_1 \cdot F_1 + \frac{F_2}{\beta_2} + \frac{F_{M1} \cdot F_{C1}}{F_1} + D_M - 2F_{C1} - F_{M1} - F_{M2} = 0, \quad (5)$$

$$\frac{F_{M1} \cdot F_{C1}}{F_1} - \frac{F_{M2} \cdot F_{C2}}{F_2} + D_M - D_C - F_{M1} - F_{C1} + F_{M2} + F_{C2} = 0, \quad (6)$$

$$\frac{F_{C2}}{F_{M2}} \cdot F_2 + \frac{F_{M1}}{F_{C1}} \cdot F_1 + \beta_2 \cdot F_2 + \frac{F_1}{\beta_1} + \frac{F_{M2} \cdot F_{C2}}{F_2} + D_I - D_M - 2F_{C2} - F_{M1} - F_{M2} = 0, \quad (7)$$

$$T = \beta_1 \cdot \beta_2. \quad (8)$$

The values D_I, D_M, D_C, F_{M1}, F_{C1}, F_{M2}, F_{C2} and T are parameters, which can be chosen appropriately. By solving equations (5) ~ (8) we can determine the values F_1, F_2, β_1 and β_2. Then, there is one configuration of the zoom part composed of thin lenses. With different value T, we can obtain different configuration.

1.2 Re-imaging

Figure 5 presents the re-imaging part of the system composed of thin lenses. E is the exit pupil of the system (constituted of X_1, M_1, C_1, M_2, C_2 and X_2), S is the cold stop of the detector. In order to satisfy 100% cold shield efficiency, the stop of the zoom optical system should be coincided with S. I_4 is the image of the point I_3. F_R is the focal length of the re-imaging part R. Imaging are given by relations,

$$\frac{1}{L_R' - D_S} - \frac{1}{L_R - D_E} = \frac{1}{F_R}, \quad (9)$$

$$\frac{1}{L_R'} - \frac{1}{L_R} = \frac{1}{F_R}, \quad (10)$$

$$\frac{L_R'}{L_R} = \beta_R, \quad (11)$$

where D_E is the distance of E from I_4, $-L_R$ is the distance of I_4 from R, L_R' is the distance of R from I_5, D_S is the distance of S from I_5, β_R is the magnification of the re-imaging part R. The values D_E, D_S and β_R are parameters, which can be chosen appropriately. By solving equations (9) ~ (11) we can determine the values F_R, L_R' and L_R. Then, there is the configuration of the re-imaging part.

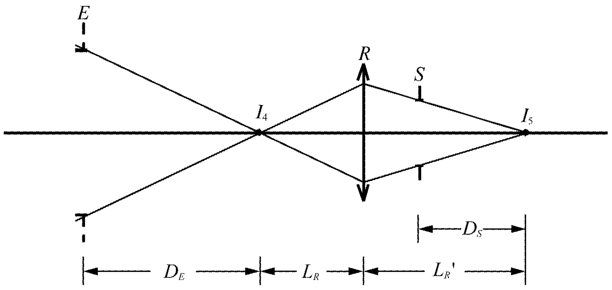

Fig. 5 Scheme of the re-imaging part
图5 光学系统二次成像部分

2 Designs

2.1 Parameters

The zoom system is with a 320×240 staring focal plane array. The dimension of detector pixel is 30 μm×30 μm. The characteristics of the system are shown in Table 1.

Table 1 Characteristics of the system
表1 系统设计指标

Focal Length Range	10 ~450 mm
Zoom Range	45
F/number	4
Spectral Band	3.7 ~4.8 μm
Field of View	1.53° ~61.92°
Operational Temperature Range	-20 ~50 ℃

2.2 Results

The zoom system was made of materials of silicon and germanium. The overall length of the system is 400 mm. In the zoom system, there are 8 lenses including 4 aspheric surfaces. Structure of the system is shown in Fig. 6. During the process of zooming, the 2nd lens and the 4th lens move together, and the 3rd lens and 5th lens also move together. Both of the paths are smooth. The zoom system satisfies 100% cold shield efficiency.

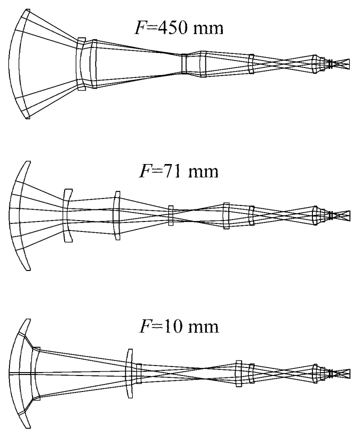

Fig. 6 Structure of the zoom system
图6 变焦系统结构图

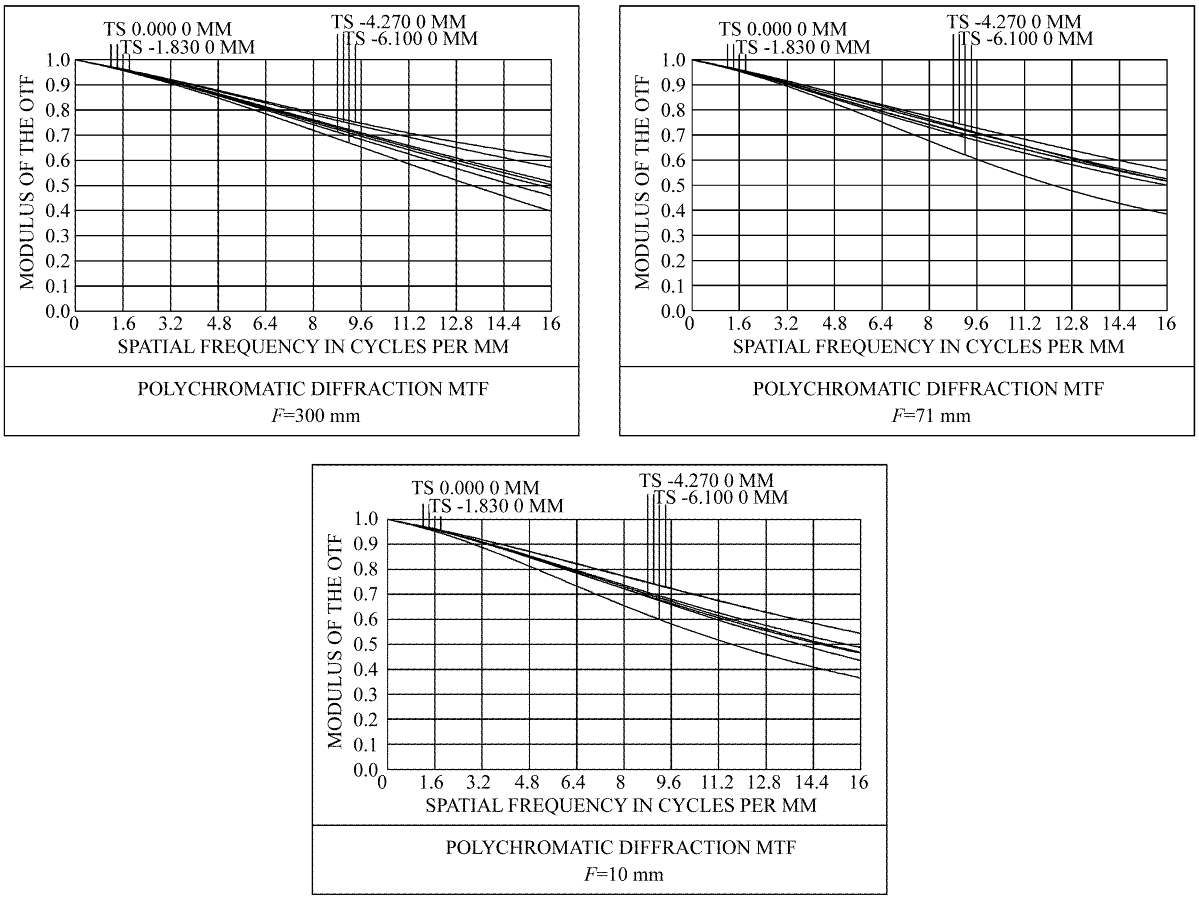

Fig. 7 MTF curves of the system
图7 系统调制传递函数图

2.3 Performance

Figure 7 illustrates MTF performances for the three different zoom positions in 20 ℃. MTF values in Nyquist limit (16 lp/mm) are more than 0.3 over the full range. It was found out that the zoom system is with high image quality. Operational temperature range of the system is −20 ~ 50 ℃, we need to achieve a thermalisation by some active means, involving temperature measurement and control of the axial position of the detector.

(下转第 77 页)

simulated S-parameters under all investigated bias conditions. In addition, the proposed method has been confirmed by the intrinsic elements, which agrees with the theoretical expectations.

REFERENCES

[1] James R. Shealy, Jiali Wang, Richard Brown. Methodology for Small-Signal Model Extraction of AlGaN HEMTs[J]. *IEEE TRANSACTRON DEVICES*, 2008, **55**(7): 1603.

[2] Campos-Roca Y, Massier H, Leuther A. Scalable HEMT Small-Signal Model Extraction based on a Hybrid Multibias Approach[J]. *IEEE MTT-S International Microwave Workshop Series on Millimeter Wave Integration Technologies*, 2011, **109**.

[3] Jianjun Gao, Xiuping Li, Hong Wang, *et al.* A New Method for Determination of Parasitic Capacitances for PHEMTs [J]. *Semicond. Sci. Technol.* 2005, **20**: 586 – 591, 587.

[4] MacFarlane D, Taking S, Murad S K, *et al.* Small Signal and Pulse Characteristics of AlN/GaN MOS-HEMTs[J]. *Proceeding of the 6th European Microwave Integrated Circuits Conference*, 342.

[5] Damian Costa, William U Liu, James S Harris. Direct Extraction of the AlGaAs/GaAs Hetero-junction Bipolar Transistor Small-Signal Equivalent Circuit[J]. *IEEE TRANSACTION ON ELECTRON DEVICE*, 1991, **38**(9): 2019 – 2020.

[6] Apolinar J Reynoso-Hernandez, Francisco Elias Rangel-Patino, Julio Perdomo. Full RF Characterization for Extracting the Small-Signal Equivalent Circuit in Microwave FET's [J]. *IEEE TRANSCATIONS ON MICROWAVE THEORY AND TECHNIQUES*, 1996, **44**(12): 2625.

[7] Giovanni Crupi, Dongping Xiao, Dominique M M -P. Schreurs. Accurate Multibias Equivalent-Circuit Extraction for GaN HEMTs[J]. *IEEE TRANSCATIONS ON MICROWAVE THEORY AND TECHNIQUES*, 2006, **54**(10): 3620.

[8] Jianjun Gao. RF and Microwave Modeling and Measurement Techniques for Field Effect Transistors[M]. *SciTech Publishing*, *Raleigh*, 2010, N. C.

(上接 71 页)

3 Conclusions

Principles of the continuous zoom system with large zoom range are introduced. A MWIR continuous zoom system with 320 × 240 staring FPA was designed, which can realize zoom range of 45. The system has high image quality and satisfies 100% cold shield efficiency. MWIR continuous zoom system with large zoom range has an enormous potential for many applications such as tracking and surveillance.

REFERENCES

[1] Sinclair R L. High Magnification Zoom Lenses for 3 ~ 5 um Applications[J]. *SPIE*, 1998, **3429**: 11 – 18.

[2] Akram M N. Design of a multiple-field-of-view optical system for 3 to 5 um infrared focal-plane arrays[J]. *Opt. Eng*, 2003, **42**(6): 1704 – 1714.

[3] Kim H S, Yu W K, Park Y C, *et al.* Compact MWIR camera with ×20 zoom optics[J]. *SPIE*, 2001, **4369**: 673 – 679.

[4] Allen Mann. Infrared Optics and Zoom Lenses[M]. *Washington*: *SPIE Press*, 2009: 45 – 53.

[5] Akram M N, Asghar M H. Step-zoom dual-field-of-view infrared telescope[J]. *Appl. Opt*, 2003, **42**(13): 2312 – 2316.

[6] Gao Hong-Yun, Xiong Tao. Mid-wavelength infrared dual field-of-view optical system[J]. *Opt. Precision Eng*(郜红云,熊涛. 中波红外两档变焦光学系统. **光学精密工程**), 2008, **16**(10): 1891 – 1894.

[7] Sanson M C, Cornell J. MWIR CONTINUOUS ZOOM WITH LARGE ZOOM RANGE[J]. *SPIE*, 2010, **7660**: 76601X – 1 – 76601X – 12.

[8] Aron Y, Boubis I, Shavit R, *et al.* Topaz – A novel design of a high magnification, athermalized 1 : 30 zoom in the MWIR[J]. *SPIE*, 2004, **5406**, 97 – 106.

[9] Porta A, Romagnoli M, Lavacchini P, *et al.* ERICA – Compact MWIR camera with ×20 step zoom optics and advanced processing[J]. *SPIE*, 2007, **6737**: 673706 – 1 – 673706 – 9.

[10] Yu Dao-Yin, Tan Heng-Ying. *Engineering Optics*[M](郁道银,谭恒英. 工程光学). *Beijing*: *Machinery Industry Press*, 2006: 22 – 26.